ARTICLE

Flexible and Transparent MoS_2 Field-Effect Transistors on Hexagonal Boron Nitride-Graphene Heterostructures

Gwan-Hyoung Lee,[†,‡,§,▼] Young-Jun Yu,[⊥,∥,▼] Xu Cui,[†] Nicholas Petrone,[†] Chul-Ho Lee,[∥,¶] Min Sup Choi,[‡,#] Dae-Yeong Lee,[‡,#] Changgu Lee,[§,#] Won Jong Yoo,[‡,#] Kenji Watanabe,[△] Takashi Taniguchi,[△] Colin Nuckolls,[¶] Philip Kim,[∥,*] and James Hone[†,*]

[†]Department of Mechanical Engineering, Columbia University, New York, New York 10027, United States, [‡]Samsung-SKKU Graphene Center (SSGC), Suwon, 440-746, Korea, [§]School of Mechanical Engineering, Sungkyunkwan University, 2066, Seobu-ro, Jangan-gu, Suwon, Gyeonggi 440-746, Korea, [⊥]Creative Research Center for Graphene Electronics, Electronics and Telecommunications Research Institute (ETRI), 218 Gajeong-ro, Yuseong-gu, Daejeon, 305-700, Korea, [∥]Department of Physics, Columbia University, New York, New York 10027, United States, [¶]Department of Chemistry, Columbia University, New York, New York 10027, United States, [#]SKKU Advanced Institute of Nano-Technology (SAINT), Sungkyunkwan University, 2066, Seobu-ro, Jangan-gu, Suwon, Gyeonggi 440-746, Korea, and [△]National Institute for Materials Science, 1-1 Namiki, Tsukuba, 305-0044, Japan. [▼]These authors contributed equally.

ABSTRACT

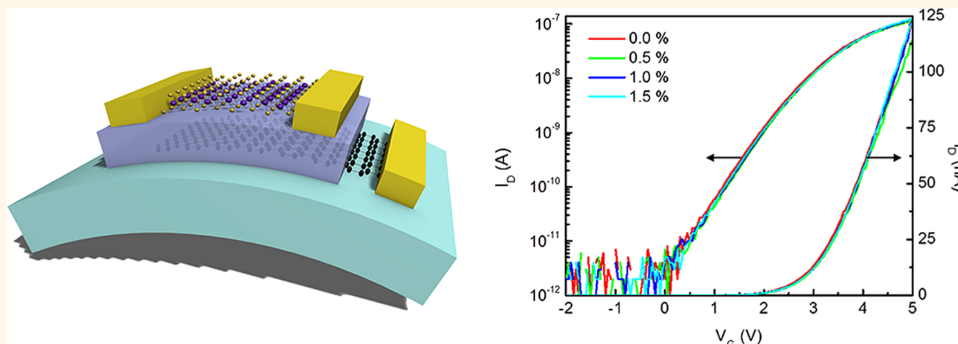

Atomically thin forms of layered materials, such as conducting graphene, insulating hexagonal boron nitride (hBN), and semiconducting molybdenum disulfide (MoS_2), have generated great interests recently due to the possibility of combining diverse atomic layers by mechanical "stacking" to create novel materials and devices. In this work, we demonstrate field-effect transistors (FETs) with MoS_2 channels, hBN dielectric, and graphene gate electrodes. These devices show field-effect mobilities of up to 45 cm^2/Vs and operating gate voltage below 10 V, with greatly reduced hysteresis. Taking advantage of the mechanical strength and flexibility of these materials, we demonstrate integration onto a polymer substrate to create flexible and transparent FETs that show unchanged performance up to 1.5% strain. These heterostructure devices consisting of ultrathin two-dimensional (2D) materials open up a new route toward high-performance flexible and transparent electronics.

KEYWORDS: molybdenum disulfide · hexagonal boron nitride · graphene · field-effect transistor · heterostructure · flexible · transparent

Recent rapid progress in basic science and applications of graphene[1−3] has been accompanied by an explosion of interest in other two-dimensional (2D) materials, such as insulating hexagonal boron nitride (hBN)[3,4] and semiconducting molybdenum disulfide (MoS_2).[5−20] MoS_2, a notable layered semiconductor among the transition metal dichalcogenide materials family, has shown interesting physical properties such as a thickness-dependent electronic band structure,[5,6] high carrier mobility,[7−9,12−17] photoconductivity,[10,11] and environmental sensitivity.[18,19] As a 2D semiconductor with excellent mechanical properties,[21] MoS_2 has great potential for flexible electronics. However, flexible MoS_2 FETs have shown relatively modest mobilities of 4−12 cm^2/Vs.[9,22] Furthermore, use of conventional dielectrics, such as SiO_2, causes large hysteresis and low mobility.[19,23,24] The hBN, which has proven to be beneficial for

* Address correspondence to pk2015@columbia.edu, jh2228@columbia.edu.

Received for review June 11, 2013 and accepted August 7, 2013.

Published online August 08, 2013
10.1021/nn402954e

© 2013 American Chemical Society

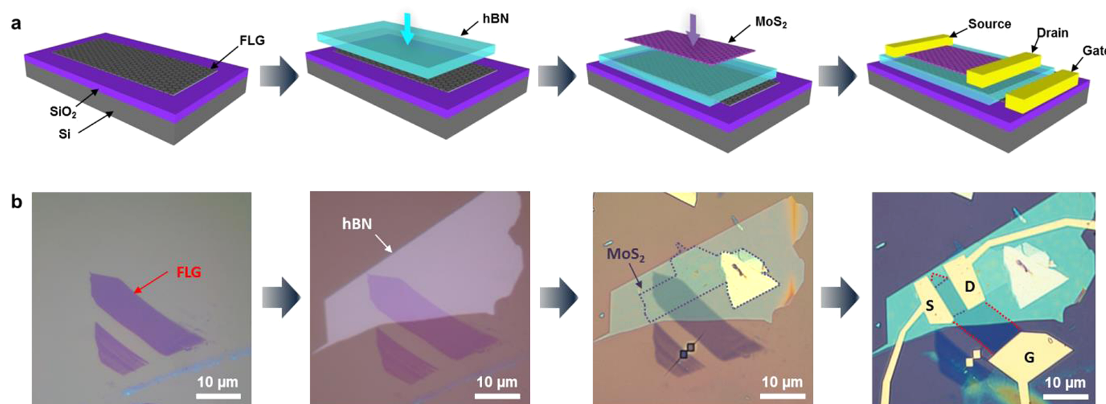

Figure 1. (a) Schematic of device fabrication process for a MBG device. (b) Optical micrographs of the corresponding samples in each fabrication step.

graphene electronics[1,25] and MoS_2 memory devices,[23] can be an alternative dielectric that is atomically flat and free of trapped charges. Finally, the inherent flexibility of 2D materials[21,26−28] motivates fabrication of flexible MoS_2 devices based on mechanically stacked heterostructures.[29,30] Here we demonstrate highly flexible and transparent MoS_2 FETs built on hBN dielectric and graphene gate electrodes, which exhibit enhanced field-effect mobility with a low operating gate voltage. The stacked heterostructure devices show high flexibility and optical transparency and exhibit little modification of device performance at high strain levels.

RESULTS AND DISCUSSION

We fabricated the FETs by mechanically stacking each layer in order on the substrate followed by e-beam lithography for electrode fabrication. Figure 1a shows the flow of fabrication processes for the complete device (MoS_2 channel, hBN dielectric, and few-layer graphene (FLG) gate), denoted below as MBG. For transfer of hBN, a polydimethylsiloxane (PDMS) stamp was used to reduce contamination on the top surface of the hBN and prevent the formation of interfacial bubbles, typically observed when polymers are used to mechanically stack 2D materials[31] (see Supporting Information, Figure S1). The MoS_2 flake was placed onto the hBN/graphene stack as described previously.[1] See Methods for details of transfer process. Source, drain, and gate electrodes were patterned by e-beam lithography and subsequent deposition of metals. Figure 1b shows optical micrographs of a representative device after each step. For the flexible devices described below, the same fabrication process was employed, except for the final annealing step (which would melt the polymer substrate). Atomic force microscopy (AFM, XE-100, Park Systems) and Raman spectroscopy (inVia, Renishaw) were employed to measure the thickness of each flake. The thickness of MoS_2 in all the tested devices was confirmed by frequency difference between in-plane $E_{2g}{}^1$ and out-of-plane A_{1g} Raman modes in the Raman spectrum as previously reported[6] (see Supporting Information, Figure S2).

To understand the effect of the hBN dielectric and graphene back-gate on FET performance, we fabricated MoS_2 FETs on SiO_2 (denoted as MS) and on SiO_2-supported hBN (denoted as MB) as depicted in Figure 2a,b. The devices were fabricated from the same monolayer MoS_2 flake to control for variability in the MoS_2 (see Supporting Information, Figure S3a). Electrical transport properties were measured with a semiconductor parameter analyzer (Agilent, 4155C) in vacuum and at room temperature. As shown in the inset of Figure 2d, linear output curves (I_D-V_D) of the MB device reveal that Ohmic contacts are formed between MoS_2 and metal electrodes as reported.[13,32] Transfer curves (I_D-V_G) of MB and MS FETs with the conducting Si wafer used as the back-gate show n-type conduction (Figure 2d). The MB device shows more than an order of magnitude increase in conductance (note that drain voltages for the MS and MB devices are different) and an order of magnitude decrease in hysteresis, providing evidence of an improved performance on hBN. This result confirms that hBN efficiently protects the MoS_2 channel from Coulomb scattering by charged impurities in the SiO_2 substrate, as previously reported for graphene FETs on hBN.[1,19]

The field-effect mobility of the devices was extracted by $\mu = (L/WC_iV_D)(dI_D/dV_G)$, where L, W, and V_G are channel length, channel width, and gate voltage, respectively. For capacitance per unit area, $C_i = \varepsilon_0\varepsilon_r/d$, relative permittivities of 3.9 and 3.5 were used for SiO_2 and hBN, respectively.[1] For monolayer MoS_2, the field-effect mobility of the MB device ($\mu_{MB} \sim 7.6$ cm^2/Vs) is an order of magnitude higher than that of MS device ($\mu_{MS} \sim 0.5$ cm^2/Vs). The on/off ratio (I_{on}/I_{off}) of both MoS_2 FETs is around 10^4-10^6, depending on the on-current.

Having confirmed the advantages of using hBN for dielectric layers, we next fabricated MBG devices, with mono- and bilayer MoS_2 channels and FLG gates (Figure 2c; see Supporting Information, Figure S3b).

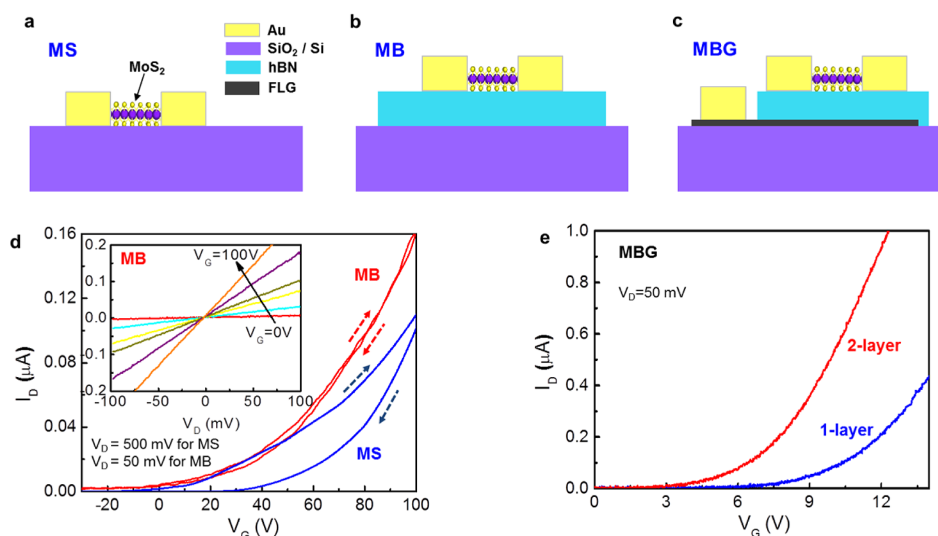

Figure 2. Schematic device structures of (a) MS, (b) MB, and (c) MBG FET. (d) Transfer curves (I_D-V_G) of MS and MB devices in (a) and (b), respectively. Note that the current (I_D) was measured with V_D of 500 and 50 mV for MS and MB, respectively. The inset of (d) shows output curves (I_D-V_D) of the MB device measured at different gate voltages with a step of 20 V. (e) Transfer curves of the MBG devices, which indicate the higher mobility of thicker MoS_2.

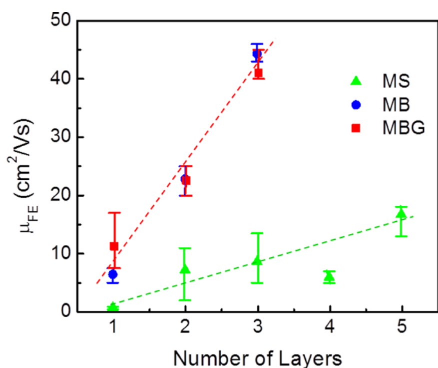

Figure 3. Field-effect mobilities of the MoS_2 FETs fabricated on different substrates as a function of number of MoS_2 layers. The solid symbols indicate average values with a distribution range from minimum to maximum. The devices with more than three, which have the same thickness of MoS_2, were measured. The dotted lines represent guidelines of mobility variation of MS, MB, and MBG devices.

Transfer curves for mono- and bilayer MoS_2 devices are shown in Figure 2e. The high-quality dielectric with smaller thickness allows low operating gate voltage (ΔV_G < 10 V) as well as higher field-effect mobilities of 12 cm^2/Vs for monolayer and 24 cm^2/Vs for bilayer MBG FETs, respectively, than those measured in MS. In addition, for MBG devices, hysteresis is completely absent, suggesting a lack of charge traps at either interface. This result confirms that hBN and graphene are well suited for use as dielectric and gate electrode materials for ultrathin MoS_2 FETs.

In order to ascertain the relation between carrier mobility and thickness of MoS_2, devices with a thickness of 1–5 layers were fabricated. The measured mobility values are summarized in Figure 3. MoS_2 FETs on both SiO_2 and hBN show increasing mobility with MoS_2 thickness, but the increase is much more dramatic on hBN substrates. Use of the graphene gate electrode does not affect mobility. Trilayer MoS_2 on hBN reaches a high mobility of ~45 cm^2/Vs, comparable to that reported for much thicker MoS_2 devices (>5 nm thick).[16] It should be noted that contact resistance is included in the two-terminal field-effect mobility estimation; the true (Hall) mobility is typically higher. A high intrinsic mobility of 470 cm^2/Vs measured by the four-terminal method was reported in 50 nm thick MoS_2.[24] The trends seen in Figure 3 are likely due to both contact and bulk effects: we have observed that the contact resistance decreases with MoS_2 thickness (unpublished data), but the observed mobility improvement on hBN indicates a substantial role of bulk scattering, at least in SiO_2-supported devices.[24] Substantial effort is now being devoted to identifying optimal contact materials for MoS_2.[20] When we compare MS and MB devices of the same MoS_2 thickness, the mobilities of MB devices are much higher than those of MS devices. For example, the mobility of monolayer MoS_2 on hBN (~10 cm^2/Vs) is an order of magnitude higher than that of monolayer MoS_2 on SiO_2 (<1 cm^2/Vs). This confirms that, although both MS and MB devices similarly show an increase of contact resistance as the MoS_2 thickness decreases, bulk scattering for thin MoS_2 is more dominant compared to contact resistance.

Based on the above results, flexible FETs were fabricated using the MBG structure with tri-layer MoS_2 to achieve high mobility, while still maintaining flexibility and optical transparency. As shown in Figure 4a, the MBG devices were fabricated on the 127 μm thick polyethylene naphthalate (PEN) substrates (DuPont Teijin Films). The representative MBG device of Figure 4b,c consists of FLG (5 layers), hBN (35 nm), and MoS_2 (3 layers). The transmission-mode optical micrograph of Figure 4c verifies that this ultrathin heterostructure

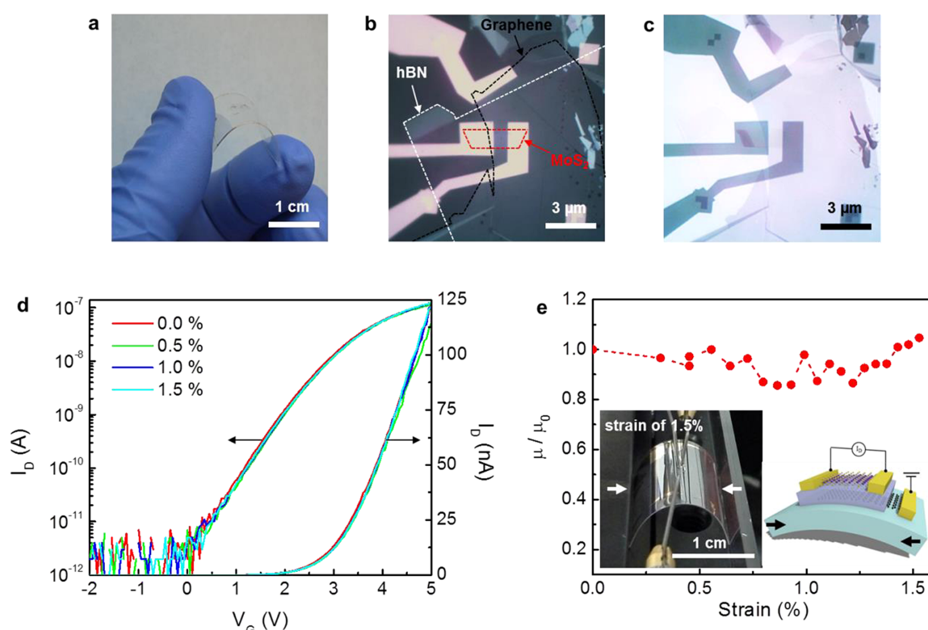

Figure 4. (a) Photograph of the MBG device on the PEN substrate showing its outstanding flexibility and transparency. (b) Reflection-mode and (c) transmission-mode optical micrographs of the flexible and transparent MBG device. Each dashed line indicates the border of each material. (d) Transfer curves of the flexible MBG device under different bending conditions up to 1.5% strain. (e) Relative field-effect mobility (μ/μ_0) of the flexible MBG device as a function of strain. The insets show the photograph of the strained MBG device by 1.5% and schematic diagram of the strained device. The arrows in the images indicate the *y*-direction for strain.

device is transparent: the optical absorption is roughly 20% for the entire device stack, as calculated from the absorption of each material (2.3% per graphene layer,[33] 2−5% for monolayer MoS_2, and negligible for hBN in visible range;[34] see Supporting Information for absorption of monolayer MoS_2, Figure S4). When only a single monolayer of each material is used, a higher transparency over 95% can be achieved, compared to 60% recently reported for multilayer MoS_2 devices.[22] Electrical device characteristics were measured under ambient conditions and different bending conditions as shown in Figure 4d. This device showed high mobility of 29 cm^2/Vs and low operating gate voltage of $\Delta V_G \sim 5$ V before bending. The smaller mobility of the MBG device on the flexible substrate is probably due to resist residue (annealing is not possible for flexible devices) and air exposure during measurement.[13,24] As was seen on rigid substrates, these samples showed no hysteresis due to the charge-trap-free hBN dielectric and clean channel/dielectric interface (see Supporting Information Figure S5).[23]

We observe that the device performance is virtually unchanged with applied uniaxial strains up to 1.5%. The sample was uniaxially strained during electrical measurements by bending, as shown in the insets of Figure 4e. The strain is calculated from the bending geometry as reported elsewhere.[35,36] The relative field-effect mobility of μ/μ_0, where μ_0 is the mobility at zero strain, is shown in Figure 4e. It is stable within 15% variation up to strain of 1.5%. The photograph in the inset of Figure 4e shows the 1.5% strained device during measurement. Above this maximum strain, most devices failed due to crack formation in the metal electrodes.[35] Even though band gap variation of MoS_2 under strain was reported,[37,38] any distinguishable change in electrical measurements of our devices was not observed.

CONCLUSIONS

In conclusion, MoS_2 FETs of a novel structure were fabricated by a mechanical stacking process with graphene and hBN. When hBN and graphene were used as dielectric and gate electrodes in MoS_2 FETs, the high field-effect mobility of 45 cm^2/Vs was achieved in trilayer MoS_2 at low operating gate voltage ($\Delta V_G < 10$ V), along with no transport curve hysteresis. We demonstrated that the heterostructure devices based on a stack of MoS_2/hBN/graphene are highly flexible and transparent. These results indicate that 2D-material-based heterostructure devices are promising for flexible and transparent electronics. For instance, this heterostructured device can be utilized in display logic circuits replacing the conventional materials (*e.g.*, amorphous Si), which require mobility larger than 10 cm^2/Vs and low power consumption.[12]

METHODS

First, graphene was mechanically exfoliated on a Si substrate with a 280 nm SiO_2 capping layer. For transfer of hBN, a polydimethylsiloxane (PDMS) stamp was placed on hBN-exfoliated Scotch tape and peeled off quickly. The PDMS-supported hBN flake (with thickness ranging from 10 to 30 nm)

was then transferred onto the FLG with a micromanipulator. Because thin MoS_2 is difficult to directly exfoliate on PDMS, MoS_2 was exfoliated on a Si chip coated by a water-soluble polymer release layer (polyvinyl acetate) and 280 nm thick poly(methyl methacrylate) (PMMA) layers. The MoS_2/PMMA film was then transferred onto a PDMS stamp by dissolving the release layer. Finally, the MoS_2 flake was placed onto the hBN/graphene stack. We note only the top surface of the final device is exposed to PMMA, so that all of the interfaces remain clean. Source, drain, and gate electrodes were patterned by e-beam lithography and subsequent deposition of Ti/Au (0.5/50 nm). For removal of PMMA residue, samples were annealed at 200 °C in vacuum.

Conflict of Interest: The authors declare no competing financial interest.

Acknowledgment. This research was supported by the U.S. National Science Foundation (DMR-1122594 and DMR-1124894). C.L. was supported by Basic Science Research Program (2011-0014209) and the Global Frontier Research Center for Advanced Soft Electronics (2011-0031629) through the National Research Foundation (NRF) funded by the Korean government Ministry of Science, ICT and Future Planning. M.S.C., D.Y.L., and W.J.Y. were supported by the Basic Science Research Program (2011-0010274 and 2013-015516) through the NRF. We thank Y. Li and T. F. Heinz for help in optical measurements.

Supporting Information Available: Additional figures. This material is available free of charge *via* the Internet at http://pubs.acs.org.

REFERENCES AND NOTES

1. Dean, C. R.; Young, A. F.; Meric, I.; Lee, C.; Wang, L.; Sorgenfrei, S.; Watanabe, K.; Taniguchi, T.; Kim, P.; Shepard, K. L.; *et al.* Boron Nitride Substrates for High-Quality Graphene Electronics. *Nat. Nanotechnol.* **2010**, *5*, 722–726.
2. Britnell, L.; Gorbachev, R. V.; Jalil, R.; Belle, B. D.; Schedin, F.; Mishchenko, A.; Georgiou, T.; Katsnelson, M. I.; Eaves, L.; Morozov, S. V.; *et al.* Field-Effect Tunneling Transistor Based on Vertical Graphene Heterostructures. *Science* **2012**, *335*, 947–950.
3. Gorbachev, R. V.; Geim, A. K.; Katsnelson, M. I.; Novoselov, K. S.; Tudorovskiy, T.; Grigorieva, I. V.; MacDonald, A. H.; Morozov, S. V.; Watanabe, K.; Taniguchi, T.; *et al.* Strong Coulomb Drag and Broken Symmetry in Double-Layer Graphene. *Nat. Phys.* **2012**, *8*, 896–901.
4. Lee, G. H.; Yu, Y. J.; Lee, C.; Dean, C.; Shepard, K. L.; Kim, P.; Hone, J. Electron Tunneling through Atomically Flat and Ultrathin Hexagonal Boron Nitride. *Appl. Phys. Lett.* **2011**, *99*, 243114.
5. Mak, K. F.; Lee, C.; Hone, J.; Shan, J.; Heinz, T. F. Atomically Thin MoS_2: A New Direct-Gap Semiconductor. *Phys. Rev. Lett.* **2010**, *105*, 136805.
6. Lee, C.; Yan, H.; Brus, L. E.; Heinz, T. F.; Hone, J.; Ryu, S. Anomalous Lattice Vibrations of Single- and Few-Layer MoS_2. *ACS Nano* **2010**, *4*, 2695–2700.
7. Zhang, Y.; Ye, J.; Matsuhashi, Y.; Iwasa, Y. Ambipolar MoS_2 Thin Flake Transistors. *Nano Lett.* **2012**, *12*, 1136–1140.
8. Wang, H.; Yu, L. L.; Lee, Y. H.; Shi, Y. M.; Hsu, A.; Chin, M. L.; Li, L. J.; Dubey, M.; Kong, J.; Palacios, T. Integrated Circuits Based on Bilayer MoS_2 Transistors. *Nano Lett.* **2012**, *12*, 4674–4680.
9. Pu, J.; Yomogida, Y.; Liu, K. K.; Li, L. J.; Iwasa, Y.; Takenobu, T. Highly Flexible MoS_2 Thin-Film Transistors with Ion Gel Dielectrics. *Nano Lett.* **2012**, *12*, 4013–4017.
10. Lee, H. S.; Min, S. W.; Chang, Y. G.; Park, M. K.; Nam, T.; Kim, H.; Kim, J. H.; Ryu, S.; Im, S. MoS_2 Nanosheet Phototransistors with Thickness-Modulated Optical Energy Gap. *Nano Lett.* **2012**, *12*, 3695–3700.
11. Yin, Z. Y.; Li, H.; Li, H.; Jiang, L.; Shi, Y. M.; Sun, Y. H.; Lu, G.; Zhang, Q.; Chen, X. D.; Zhang, H. Single-Layer MoS_2 Phototransistors. *ACS Nano* **2012**, *6*, 74–80.
12. Kim, S.; Konar, A.; Hwang, W. S.; Lee, J. H.; Lee, J.; Yang, J.; Jung, C.; Kim, H.; Yoo, J. B.; Choi, J. Y.; *et al.* High-Mobility and Low-Power Thin-Film Transistors Based on Multilayer MoS_2 Crystals. *Nat. Commun.* **2012**, *3*, 1011.
13. Radisavljevic, B.; Radenovic, A.; Brivio, J.; Giacometti, V.; Kis, A. Single-Layer MoS_2 Transistors. *Nat. Nanotechnol.* **2011**, *6*, 147–150.
14. Radisavljevic, B.; Whitwick, M. B.; Kis, A. Intergrated Circuits and Logic Operations Based on Single-Layer MoS_2. *ACS Nano* **2011**, *5*, 9934–9938.
15. Yoon, Y.; Ganapathi, K.; Salahuddin, S. How Good Can Monolayer MoS_2 Transistors Be? *Nano Lett.* **2011**, *11*, 3768–3773.
16. Ayari, A.; Cobas, E.; Ogundadegbe, O.; Fuhrer, M. S. Realization and Electrical Characterization of Ultrathin Crystals of Layered Transition-Metal Dichalcogenides. *J. Appl. Phys.* **2007**, *101*, 014507.
17. Ghatak, S.; Pal, A. N.; Ghosh, A. Nature of Electronic States in Atomically Thin MoS_2 Field-Effect Transistors. *ACS Nano* **2011**, *5*, 7707–7712.
18. Qiu, H.; Pan, L. J.; Yao, Z. N.; Li, J. J.; Shi, Y.; Wang, X. R. Electrical Characterization of Back-Gated Bi-layer MoS_2 Field-Effect Transistors and the Effect of Ambient on Their Performances. *Appl. Phys. Lett.* **2012**, *100*, 123104.
19. Late, D. J.; Liu, B.; Matte, H. S. S. R.; Dravid, V. P.; Rao, C. N. R. Hysteresis in Single-Layer MoS_2 Field Effect Transistors. *ACS Nano* **2012**, *6*, 5635–5641.
20. Das, S.; Chen, H. Y.; Penumatcha, A. V.; Appenzeller, J. High Performance Multilayer MoS_2 Transistors with Scandium Contacts. *Nano Lett.* **2013**, *13*, 100–105.
21. Cooper, R. C.; Lee, C.; Marianetti, C. A.; Wei, X. D.; Hone, J.; Kysar, J. W. Nonlinear Elastic Behavior of Two-Dimensional Molybdenum Disulfide. *Phys. Rev. B* **2013**, *87*, 035423.
22. Yoon, J.; Park, W.; Bae, G. Y.; Kim, Y.; Jang, H. S.; Hyun, Y.; Lim, S. K.; Kahng, Y. H.; Hong, W. K.; Lee, B. H.; *et al.* Highly Flexible and Transparent Multilayer MoS_2 Transistors with Graphene Electrodes. *Small* **2013**, 10.1002/smll.201300134.
23. Choi, M. S.; Lee, G. H.; Yu, Y. J.; Lee, D. Y.; Lee, S. H.; Kim, P.; Hone, J.; Yoo, W. J. Controlled Charge Trapping by Molybdenum Disulphide and Graphene in Ultrathin Heterostructured Memory Devices. *Nat. Commun.* **2013**, *4*, 1624.
24. Bao, W. Z.; Cai, X. H.; Kim, D.; Sridhara, K.; Fuhrer, M. S. High Mobility Ambipolar MoS_2 Field-Effect Transistors: Substrate and Dielectric Effects. *Appl. Phys. Lett.* **2013**, *102*, 042104.
25. Dean, C.; Young, A. F.; Wang, L.; Meric, I.; Lee, G. H.; Watanabe, K.; Taniguchi, T.; Shepard, K.; Kim, P.; Hone, J. Graphene Based Heterostructures. *Solid State Commun.* **2012**, *152*, 1275–1282.
26. Lee, C.; Wei, X. D.; Kysar, J. W.; Hone, J. Measurement of the Elastic Properties and Intrinsic Strength of Monolayer Graphene. *Science* **2008**, *321*, 385–388.
27. Liu, Z.; Ma, L. L.; Shi, G.; Zhou, W.; Gong, Y. J.; Lei, S. D.; Yang, X. B.; Zhang, J. N.; Yu, J. J.; Hackenberg, K. P.; *et al.* In-Plane Heterostructures of Graphene and Hexagonal Boron Nitride with Controlled Domain Sizes. *Nat. Nanotechnol.* **2013**, *8*, 119–124.
28. Lee, G. H.; Cooper, R. C.; An, S. J.; Lee, S.; van der Zande, A.; Petrone, N.; Hammerberg, A. G.; Lee, C.; Crawford, B.; Oliver, W.; *et al.* High-Strength Chemical-Vapor-Deposited Graphene and Grain Boundaries. *Science* **2013**, *340*, 1073–1076.
29. Georgiou, T.; Jalil, R.; Belle, B. D.; Britnell, L.; Gorbachev, R. V.; Morozov, S. V.; Kim, Y. J.; Gholinia, A.; Haigh, S. J.; Makarovsky, O.; *et al.* Vertical Field-Effect Transistor Based on Graphene−WS_2 Heterostructures for Flexible and Transparent Electronics. *Nat. Nanotechnol.* **2013**, *8*, 100–103.
30. Britnell, L.; Ribeiro, R. M.; Eckmann, A.; Jalil, R.; Belle, B. D.; Mishchenko, A.; Kim, Y.-J.; Gorbachev, R. V.; Georgiou, T.; Morozov, S. V.; *et al.* Strong Light−Matter Interactions in Heterostructures of Atomically Thin Films. *Science* **2013**, *340*, 1311–1314.
31. Haigh, S. J.; Gholinia, A.; Jalil, R.; Romani, S.; Britnell, L.; Elias, D. C.; Novoselov, K. S.; Ponomarenko, L. A.; Geim, A. K.; Gorbachev, R. Cross-Sectional Imaging of Individual Layers and Buried Interfaces of Graphene-Based Heterostructures and Superlattices. *Nat. Mater.* **2012**, *11*, 764–767.

32. Liu, H.; Neal, A. T.; Ye, P. D. Channel Length Scaling of MoS_2 MOSFETs. *ACS Nano* **2012**, *6*, 8563–8569.
33. Nair, R. R.; Blake, P.; Grigorenko, A. N.; Novoselov, K. S.; Booth, T. J.; Stauber, T.; Peres, N. M. R.; Geim, A. K. Fine Structure Constant Defines Visual Transparency of Graphene. *Science* **2008**, *320*, 1308–1308.
34. Remes, Z.; Nesladek, M.; Haenen, K.; Watanabe, K.; Taniguchi, T. The Optical Absorption and Photoconductivity Spectra of Hexagonal Boron Nitride Single Crystals. *Phys. Status Solidi A* **2005**, *202*, 2229–2233.
35. Petrone, N.; Meric, I.; Hone, J.; Shepard, K. L. Graphene Field-Effect Transistors with Gigahertz-Frequency Power Gain on Flexible Substrates. *Nano Lett.* **2013**, *13*, 121–125.
36. Scarpello, G. M.; Ritelli, D. Elliptic Integral Solutions of Spatial Elastica of a Thin Straight Rod Bent under Concentrated Terminal Forces. *Meccanica* **2006**, *41*, 519–527.
37. Conley, H. J.; Wang, B.; Ziegler, J. I.; Haglund, R. F., Jr.; Pantelides, S. T.; Bolotin, K. I. Bandgap Engineering of Strained Monolayer and Bilayer MoS_2. *Nano Lett.* **2013**, 10.1021/nl4014748.
38. He, K.; Poole, C.; Mak, K. F.; Shan, J. Experimental Demonstration of Continuous Electronic Structure Tuning *via* Strain in Atomically Thin MoS_2. *Nano Lett.* **2013**, *13*, 2931–2936.